PHYSICAL REVIEW B VOLUME 26, NUMBER 1 1 JULY 1982

Atomic rearrangements and crystalline transformations in amorphous $Fe_{81}B_{13.5}Si_{3.5}C_2$

N. Saegusa and A. H. Morrish
Department of Physics, University of Manitoba, Winnipeg, Manitoba R3T 2N2, Canada
(Received 16 February 1982)

Atomic rearrangements and amorphous-to-crystalline transformations after isochronal annealing of as-quenched $Fe_{81}B_{13.5}Si_{3.5}C_2$ (METGLAS® 2605SC) have been investigated by Mössbauer spectroscopy. The atomic rearrangements in the amorphous state consist of two major processes that depend on the annealing temperature. The first process is attributed to enhancement of the short-range order and the second one to the atomic rearrangements leading to crystallization. The crystallization was found to consist of at least two steps. In the first step, precipitation of Fe—4 at. % Si alloy takes place. The final crystalline products are Fe—7 at. % Si, Fe_2B, and Fe_3C. Just before crystallization occurs, the ^{57}Fe Mössbauer recoilless fraction, f, increases by 8%, and, after the completion of crystallization, the f factor increases by 29%, both as compared to the as-quenched amorphous alloy.

I. INTRODUCTION

The amorphous-to-crystalline transformation of metallic glasses has been the subject of recent studies. For the binary amorphous alloy, $Fe_{1-x}B_x$, two types of crystallization processes have been reported. For boron concentrations less than 16 at. % the crystallization takes place in two steps, whereas for boron concentrations more than 16 at. % the crystallization occurs in a single step.[1] For $x < 0.16$, the first step is a precipitation of α-Fe until the composition of the remaining glassy state transforms into metastable Fe_3B that then decomposes into α-Fe and Fe_2B at higher temperatures.[1] For $x > 0.16$, crystallization takes place by the eutectic type of reaction in which the two crystalline phases, α-Fe and Fe_3B, are produced from the beginning, in a ratio that remains constant throughout the transformation.[1,2] Recently a two-step crystallization process was observed for the ternary amorphous alloy, $Fe_{82}B_{12}Si_6$.[3] In addition, atomic rearrangements that occur before the onset of crystallization have been reported.[2,3]

The transformation of the quaternary amorphous alloy $Fe_{81}B_{13.5}Si_{3.5}C_2$ (METGLAS® 2605SC) from the as-quenched amorphous to the crystalline state has been investigated recently in our laboratory by Mössbauer spectroscopy. The annealing-temperature dependences of the Mössbauer parameters were analyzed in order to study the changes in the amorphous-to-crystalline transformations and the preceding atomic rearrangements. These depend on both the annealing time and temperature. This paper deals with the effects observed for isochronal annealing.

II. EXPERIMENTAL

Amorphous $Fe_{81}B_{13.5}Si_{3.5}C_2$ (METGLAS® 2605SC) in a continuous ribbon form of 25.4-mm width and nominally 30-μm thickness was obtained from the Allied Corporation, USA. Samples for annealing were cut from the ribbon; typically the size was about 25.4×8 mm^2. The annealing time at temperatures between 350 and 995 K was arbitrarily chosen to be 20 min. A conventional tube furnace, fitted with a glass insert to allow circulating He gas, was used for the annealing. The typical heating-up time to the annealing temperature T_A from room temperature was about 20 min for temperatures up to 760 K. Above 760 K, the heating-up time was longer, e.g., 50 min for $T_A = 995$ K. Cool down from the annealing temperature to room temperature took about 10 min. The annealing temperature was monitored with a Chromel-Alumel thermocouple placed close to the sample.

Mössbauer measurements at room temperature were made with a conventional constant-acceleration spectrometer using a sawtooth-drive wave form and a 512 channel analyzer. The γ-ray source was ^{57}Co in Rh matrix kept at room temperature. The number of counts recorded ranged between 2.6×10^6 and 3.1×10^6 counts per channel for the isochronally annealed samples.

In addition, some Mössbauer spectra were recorded above room temperature using a vacuum furnace with a temperature stability lying within ± 0.5 K over 24 h. For these spectra, the number of counts ranged between 0.45×10^6 and 2.1×10^6 counts per channel.

Also, one spectrum was taken with an external magnetic field of 5.0 T applied parallel to the γ-ray propagation direction. This field was produced by a superconducting solenoid with a room-temperature access space.

The absorption lines of the amorphous phase were fitted with quasi-Lorentzian line shapes[4] used previously.[5] The only constraint applied was that $A_1=A_6$, $A_2=A_5$, and $A_3=A_4$, where A_i represents the absorption area of ith absorption line, as expected for the 14.4-keV γ-ray transition of ^{57}Fe.[6] Lorentzian line shapes were used to fit the patterns of the crystalline phases. To aid in the fitting, the patterns for the crystalline components were constrained to ratios of $A_1:A_2:A_3::3:2:1$, which are the values for random orientation of the magnetization.[6] Also, the linewidths Γ_i $(i=1,2,\ldots,6)$ were constrained to be

$$\Gamma_1:\Gamma_2:\Gamma_3:\Gamma_4:\Gamma_5\Gamma_6::1:0.92:0.89:0.89:0.92:1\ ,$$

which corresponds to the ratio of the linewidths observed with the spectrometer for a 6.4-μm thick α-Fe foil.

III. RESULTS AND DISCUSSION

Figure 1 shows selected transmission ^{57}Fe Mössbauer spectra taken at room temperature for samples annealed at various temperatures with $T_A \leq 685$ K, together with a spectrum for the as-

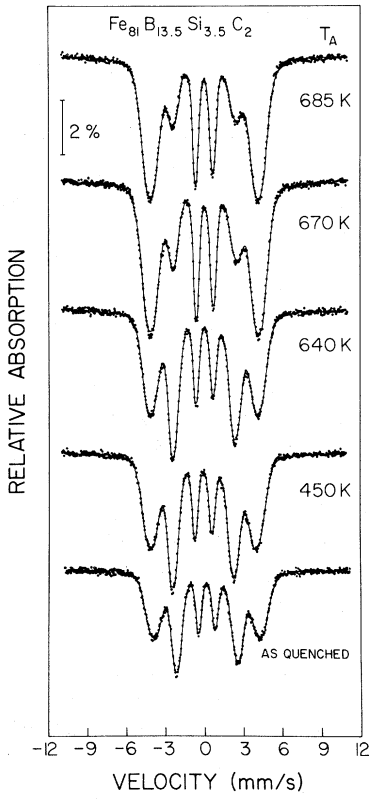

FIG. 1. Transmission Mössbauer spectra at room temperature of amorphous $Fe_{81}B_{13.5}Si_{3.5}C_2$ after annealing at various temperatures T_A for 20 min. The spectrum of an as-quenched sample is also displayed at the bottom of the figure.

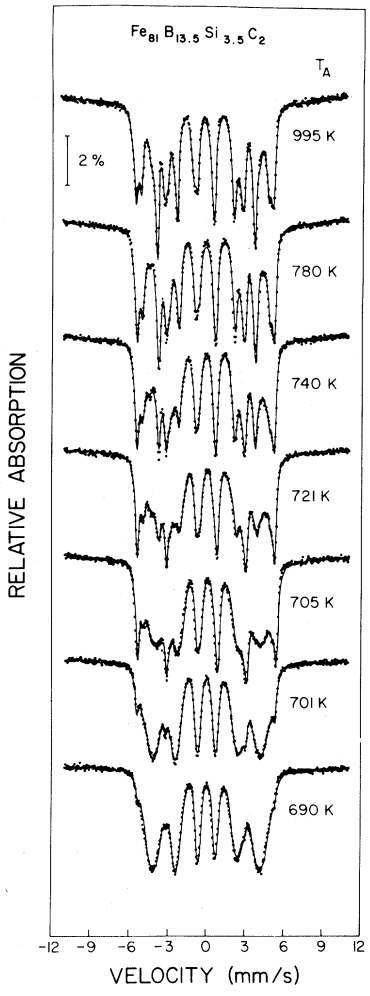

FIG. 2. Mössbauer spectra at room temperature of isochronally annealed $Fe_{81}B_{13.5}Si_{3.5}C_2$ samples for T_A between 690 and 995 K.

quenched alloy. All these spectra consist of six broadened lines. However, as the annealing temperature, T_A, is raised above 685 K, narrow lines, presumably corresponding to crystalline phases, appear, as shown in Fig. 2. For $T_A \geq 780$ K, the amorphous pattern appears to be absent, and each spectrum consists of at least four six-line patterns.

A. Completely crystallized ribbon

Hyperfine parameters obtained from the computer fitting to the spectra for $T_A \geq 780$ K are given in Table I. In order to identify the crystalline products, possible crystalline compounds and alloys that may be produced from amorphous Fe-B-Si-C alloys are listed in Table II.[7–14] A comparison of the hyperfine parameters in Tables I and II suggests that the first three patterns are for Fe-Si alloy and the fourth one for Fe_2B.

It is to be noted that no crystalline products containing carbon were identified. Possible reasons are that (a) the crystalline products containing carbon do not contain iron and (b) any patterns for crystalline products containing both carbon and iron overlap the other patterns and are not resolved. In order to clarify this point, a Mössbauer spectrum of the sample annealed at 850 K was recorded at room temperature in an external magnetic field of 5.0 T applied parallel to the γ-ray propagation direction. For a ferromagnet with a collinear magnetic structure in this geometry, the second and fifth Mössbauer lines will be absent,[6] and hence assist in resolving the remaining lines. The spectrum obtained is shown in Fig. 3. Five doublets were fitted to the outermost two (first and sixth) lines. The hyperfine fields were obtained from the separation of these outermost lines, and are listed in Table III. The corresponding hyperfine fields in zero external field are expected to differ by about ± 5 T as compared to the values given in Table III. On the basis of these hyperfine fields, and also on considering the relative absorption areas, it is reasonable to assign the first three patterns to Fe-Si alloy and the fourth to Fe_2B.

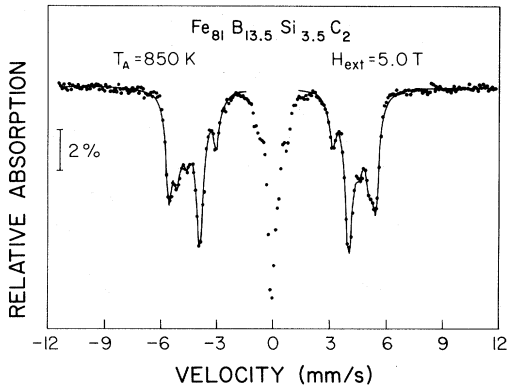

FIG. 3. Room-temperature spectrum of $Fe_{81}B_{13.5}Si_{3.5}C_2$ annealed at $T_A = 850$ K with an external magnetic field of 5.0 T applied parallel to the γ-ray propagation direction.

TABLE I. Hyperfine parameters and relative areas for patterns of four crystalline phases after annealing amorphous $Fe_{81}B_{13.5}Si_{3.5}C_2$ at various annealing temperatures for 20 min.

T_A (K)		Pattern 1	Pattern 2	Pattern 3	Pattern 4
995	H_{hf} (T)	33.21	30.81	26.35	23.66
	δ (mm/s)	0.020	0.057	0.099	0.126
	relative area (%)	25	23	12	39
900	H_{hf} (T)	33.20	30.81	27.08	23.59
	δ (mm/s)	0.013	0.005	0.081	0.110
	relative area (%)	28	23	7	42
850	H_{hf} (T)	33.16	30.79	27.31	23.54
	δ (mm/s)	0.005	0.044	0.043	0.114
	relative area (%)	28	22	6	44
800	H_{hf} (T)	33.21	30.80	27.67	23.53
	δ (mm/s)	−0.001	0.038	0.089	0.106
	relative area (%)	29	22	4	45
780	H_{hf} (T)	33.18	30.70	27.33	23.48
	δ (mm/s)	0.025	0.063	0.071	0.131
	relative area (%)	30	22	5	43

TABLE II. Data on stable crystalline materials that may be phases produced during crystallization of amorphous $Fe_{81}B_{13.5}Si_{3.5}C_2$. The isomer shifts δ are relative to α-Fe foil.

Crystalline material	Structure	Site	H_{hf} (T)	δ (mm/s)	Ref.
α-Fe	bcc		33.04	0.0	a
FeB	orthorhombic		11.8	0.28	b
Fe_2B	tetragonal		23.7	0.12	c
Fe_3B	tetragonal		~30.0		d
			~27.5		
			~23.0		
Fe_3Si	DO_3	*A*	20.1	0.26	e
		D	31.0	0.08	
Fe_5SiB_2	tetragonal	Fe(1)[a]	17.0	0.28	f
		Fe(1)[b]	19.8	0.28	
		Fe(2)	23.0	0.12	
Fe-6.7 at.% Si	bcc	8 Fe NN	33.31	0.02	g
		7 Fe NN	30.92	0.05	
		6 Fe NN	28.24	0.09	
Fe_3C	orthorhombic		20.8	0.29	h
Fe_5C_2	orthorhombic	Fe(1)	22.2	0.35	h
		Fe(2)	18.4	0.30	
		Fe(3)	11.0	0.30	

[a] Reference 7.
[b] Reference 8.
[c] Reference 9.
[d] Reference 10.
[e] Reference 11.
[f] Reference 12.
[g] Reference 13.
[h] Reference 14.

Assignment of the fifth pattern is made to Fe_3C, which has a hyperfine field of 20.8 T at $T=295$ K.[14] This identification is strengthened by conversion-electron Mössbauer spectra, which appear to show the presence of Fe_3C in the surface layers of the same annealed samples.[15] Further support comes from Arajs *et al.*,[16] who concluded that $Fe_3(B,C)$ forms after annealing amorphous Fe-B-C.

The silicon concentration c in the Fe-Si alloy

TABLE III. Proposed identification of five Mössbauer patterns after amorphous $Fe_{81}B_{13.5}Si_{3.5}C_2$ had been annealed at 850 K for 20 min. Here FWHM denotes the full width at half-maximum of the outermost (first and sixth) lines.

Mössbauer pattern	H_{hf} (T)	δ (mm/s)	FWHM (mm/s)	Relative area (%)	Assignment
1	34.16	−0.08	0.40	19.0	Fe-Si 8 NN
2	31.77	−0.03	0.47	16.1	Fe-Si 7 NN
3	28.51	−0.04	0.63	16.5	Fe-Si 6 NN
4	24.54	0.04	0.51	38.0	Fe_2B
5	19.08	0.04	0.44	10.4	Fe_3C

was estimated by assuming that Si atoms are distributed randomly at bcc lattice sites. The probability for an iron atom to have l Fe nearest neighbors is then given by the equation

$$P(c,l)=\begin{bmatrix}8\\l\end{bmatrix}(1-c)^l c^{8-l}, \quad (1)$$

and some values are tabulated in Table IV. Comparison of Table IV with the data for $T_A=780$ and 800 K (Table I) shows that the intensity ratio corresponding to a Si concentration of 7 at. % is closest.

As is evident in Fig. 2, the overall shape of a spectrum changes even after the completion of crystallization. No new patterns were fitted for $T_A > 800$ K. As may be seen from Table I, a change in the relative areas of the patterns occurs for the 8 Fe NN, 7 Fe NN, and 6 Fe NN components of the Fe-Si alloy where NN means nearest neighbor. Therefore, as the annealing temperature is raised above about 800 K, ordering develops in the Fe-Si alloy; a similar result was observed for amorphous $Fe_{82}B_{12}Si_6$.[3]

An estimate of the atomic composition of the amorphous state may be made by starting with the crystalline products as identified, then by considering their relative absorption areas (Table III), and by assuming that their recoilless fractions at room temperature are all the same. This calculation yields the atomic composition as $Fe_{79.1}B_{15.0}Si_{3.1}C_{2.8}$. Since the error in the determination of the absorption areas is $\pm 3\%$, and in addition the recoilless fractions may indeed be different at room temperature, this composition is satisfactorily close to the nominal one, $Fe_{81}B_{13.5}Si_{3.5}C_2$, given by the manufacturer. This result therefore provides some confidence that the final crystallization products have been correctly identified.

TABLE IV. Occupation probabilities for a random distribution of silicon in Fe-Si alloy. Here c is the Si concentration (%) and l is the number of Fe nearest neighbors (NN) to a certain iron site.

c (%) \ l	8	7	6
1	92	8	0
2	85	14	1
3	78	19	3
4	72	24	4
5	66	28	6
6	61	31	8
7	57	34	9
8	52	36	11
9	48	38	13
10	45	40	15

B. Amorphous-to-crystalline transformation

In the isochronal annealing experiments, the onset of crystallization is first clearly observed for $T_A=690$ K (see Fig. 2). Two patterns associated with this initial crystallization are fitted, and have hyperfine fields of 33.08 and 30.91 T. The pattern with the lower hyperfine field completely overlaps that for the amorphous component, and hence the accuracy of fitting is not good. In view of the identification of the products for complete crystallization, it is tempting to ascribe the initial crystallization to an Fe-Si alloy. However, on the basis of x-ray diffraction, Swartz *et al.*[17] proposed that the first crystalline phase to precipitate is α-Fe; indeed α-Fe has a hyperfine field at room temperature of 33.04 ± 0.03 T.[7]

In order to clarify this question, further experiments were conducted in which attempts were made to increase the amount of the initial crystalline phase present. A sample was heated from room temperature to 670 K in successively increasing temperature steps over the period of about one week. Spectra were then recorded at $T=670$ K and at successively lower temperatures; some are shown in Fig. 4. The uppermost spectrum was taken in a 4-h period immediately upon reaching 670 K, and the second spectrum was taken over a 12-h period starting 12 h after reaching 670 K. The spectra at 600, 500, and 297 K were each recorded for a 12-h period during the cool down. For comparison purposes, an as-quenched sample was quickly heated to 670 K and then maintained at this temperature for 3 d: the resulting spectrum was intermediate to the two for 670 K in Fig. 4. Finally, it should be noted that the room-temperature spectrum for $T_A=705$ K (Fig. 2) is similar to that for 297 K in Fig. 4.

Three patterns, two for the crystalline and one for the amorphous components, were fitted to the spectra of Fig. 4; some of the hyperfine parameters obtained are listed in Table V. The increase in the absorption areas for the patterns associated with the crystalline phase shows that once crystallization is nucleated, further growth occurs even at re-

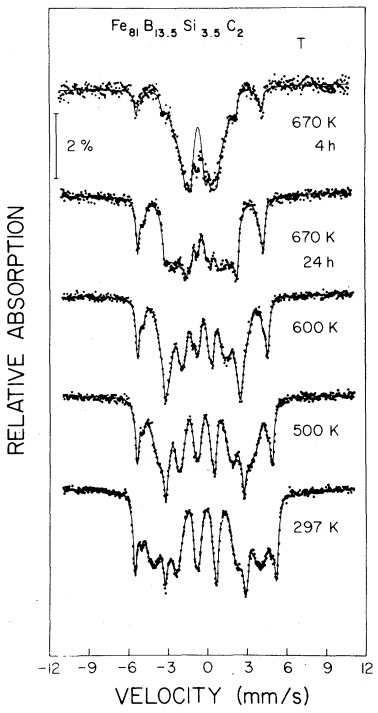

FIG. 4. Mössbauer spectra of $Fe_{81}B_{13.5}Si_{3.5}C_2$ at elevated temperatures. The topmost spectrum was recorded for 4 h immediately after the sample was heated to 670 K. For the spectrum second from the top, the sample were annealed at 670 K for 12 h and then the data was collected over the ensuing 12 h. The last three spectra were obtained after cooling the sample from 670 K; the collection time for each spectrum was about 24 h.

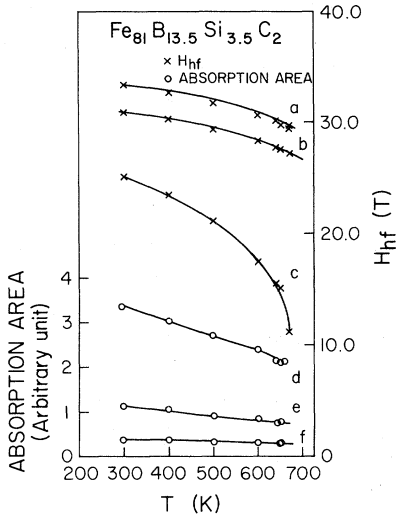

FIG. 5. Temperature dependence of the hyperfine field and absorption area for the spectra of Fig. 4. Here *a* and *e* are for crystalline Fe-Si with 8 NN, *b* and *f* are for crystalline Fe-Si with 7 NN, and *c* and *d* for the amorphous component.

latively low temperatures.

The temperature dependence of the hyperfine fields and the absorption areas for the three patterns (fitted to the spectra of Fig. 4, and others not shown) are plotted in Fig. 5. The general continuity of the data indicates that only two crystalline patterns are present. If one pattern is for α-Fe, it does not seem possible that the other is for an Fe-Si alloy. Instead, it is much more likely that both patterns are for an Fe-Si alloy, one for an iron atom with 8 Fe NN and the other with 7 Fe NN. The absence of a third pattern corresponding to Fe with 6 Fe NN, as observed after complete crystallization, indicates that the silicon concentration in the early stages of precipitation is smaller. For the spectrum at 297 K in Fig. 4, a Si concentration of about 4 at. % best fits the data.

It should be pointed out that the recoilless fractions, f, of the amorphous and crystalline phases

TABLE V. Parameters obtained for three spectra of Fig. 4 for the amorphous state and crystalline Fe-Si alloy with 8 and 7 nearest neighbors (NN).

Temperature (K)	Parameter	Fe-Si 8 NN	Fe-Si 7 NN	Amorphous component
670[a]	H_{hf} (T)	29.68	27.34	10.72
	relative area (%)	12	6	82
670[b]	H_{hf} (T)	29.58	27.24	10.85
	relative area (%)	15	6	79
297	H_{hf} (T)	33.70	30.91	25.24
	relative area (%)	23	8	69

[a] Spectrum recorded for 4 h after reaching $T=670$ K.

[b] Spectrum recorded for 12 h after a 12-h annealing at $T=670$ K.

may be different at room temperature. Figure 6 shows the dependence of the total absorption area, (proportional to f) on the annealing temperature, T_A, as determined from the room-temperature spectra of Figs. 1 and 2. For the sample annealed at 685 K, and assumed to be still in the amorphous state, the total absorption increases by 8% over that for the as-quenched sample. For the completely crystallized state ($T_A > 800$ K), the total absorption area increases by 29% as compared to that for the as-quenched ribbon. Therefore, the actual abundance of the crystalline phase may be as much as 29% less than that given by the relative absorption areas of the amorphous and crystalline phases.

The pattern for the amorphous phase in the spectra at $T=670$ K in Fig. 4 has magnetic hyperfine splitting. In other words, this amorphous phase is magnetically ordered, even though the Curie temperature determined by a thermal scan of an as-quenched ribbon is 668 K.[5] Now, in general when the magnetization of an iron-containing amorphous alloy is decreased, an increase in the ordering temperature is observed.[18] Further, in particular as shown in Fig. 7, the hyperfine field, which is proportional to the magnetization, does decrease after the onset of crystallization in $Fe_{81}B_{13.5}Si_{3.5}C_2$. Therefore, it is reasonable to attribute the increase in the Curie temperature (Fig. 4) to a reduction in the iron concentration in the amorphous component after the precipitation of the crystalline Fe-Si alloy.

The relative areas of the Mössbauer patterns for the spectra of Fig. 2 are plotted as a function of the annealing temperature in Fig. 8. Because the recoilless fractions of the amorphous and crystalline phases differ, the relative abundance of the crystalline phases will be smaller than indicated by the relative areas. At $T_A \approx 715$ K, the Fe_2B phase starts to crystallize.

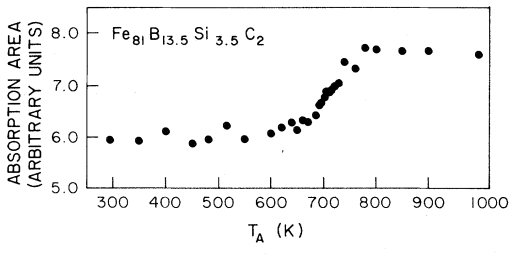

FIG. 6. Total absorption area for $Fe_{81}B_{13.5}Si_{3.5}C_2$ at room temperature as a function of the annealing temperature.

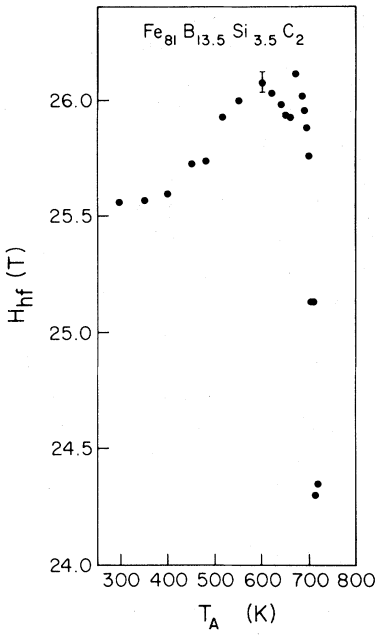

FIG. 7. Hyperfine field of the amorphous component determined at room temperature vs the annealing temperature. The bar at the datum point at 600 K shows the typical error associated with the experimental uncertainties.

From Fig. 8, it may be noted that the relative areas are relatively constant for T_A between 705 and 710 K and also between 715 and 730 K. One similar plateau in the relative areas was observed for $Fe_{82}B_{12}Si_6$, and was attributed to the formation of a quasistable amorphous state in which the ratio of transition-metal to metalloid atoms is approximately 3 to 1.[3]

The atomic compositions of the quasistable amorphous phases for $Fe_{81}B_{13.5}Si_{3.5}C_2$ may be estimated by assuming that the recoilless fractions of

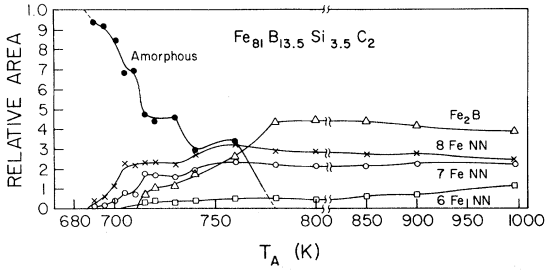

FIG. 8. Annealing temperature dependence of the relative absorption area for the amorphous and crystalline phases determined from room-temperature spectra.

the amorphous and crystalline states are 8% and 29% larger, respectively, than the f factor of the as-quenched amorphous alloy. Then the relative areas of the amorphous and crystalline phases are calculated to be in the ratio of 73.6:26.4. The first plateau ($705 \leq T_A \leq 710$ K) appears to begin just after the precipation of crystalline Fe—4 at. % Si; the atomic composition then calculated for the amorphous phase is $Fe_{75.2}B_{18.6}Si_{3.4}C_{2.8}$. For the second plateau ($715 \leq T_A \leq 730$ K), on the assumption that its onset follows the precipitation of crystalline Fe—7 at. % Si and Fe_2B, the amorphous phase composition is determined to be $Fe_{76.0}B_{17.3}Si_{3.0}C_{3.7}$. If, in addition, Fe_3C has completely crystallized out, the amorphous composition is found to be $Fe_{76.2}B_{20.3}Si_{3.5}$. Indeed, it is possible that the presence of two quasistable regions as compared to only one observed for the ternary amorphous alloy $Fe_{82}B_{12}Si_6$ is related to the additional Fe_3C crystalline component. As is evident from Figs. 2 and 8, above $T_A = 730$ K the crystallization continues until it is completed at about $T_A = 780$ K.

The area ratios of the Mössbauer lines for the amorphous phase associated with the spectra of Figs. 1 and 2 are shown in Fig. 9. Here $A_{i,j}$ is the area for line i or j. For $690 \leq T_A \leq 740$ K, $A_{2,5}/A_{1,6} \approx 0.7$, and is close to the value of 0.67 corresponding to random orientation of the magnetic moments with respect to the γ-ray propagation direction.[6]

The ratio $A_{2,5}/A_{1,6}$ begins to decrease at about $T_A = 630$ K and reaches a minimum at $T_A \approx 685$ K

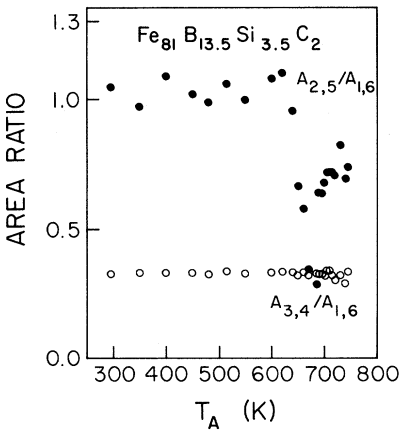

FIG. 9. Annealing temperature dependence of the relative area $A_{2,5}/A_{1,6}$ and $A_{3,4}/A_{1,6}$ of the amorphous component of $Fe_{81}B_{13.5}Si_{3.5}C_2$, obtained from room-temperature spectra.

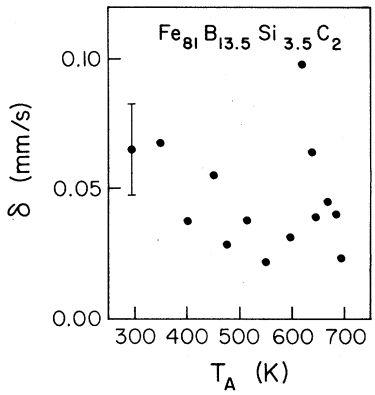

FIG. 10. Isomer shift vs annealing temperature for the amorphous component of $Fe_{81}B_{13.5}Si_{3.5}C_2$ measured at room temperature.

(Fig. 9). Hence, in this annealing-temperature range the average magnetic-moment direction changes from close to parallel to almost perpendicular to the ribbon plane as T_A is increased. Now, as shown in Fig. 1, no crystallization is observed for $T_A < 690$ K. However, conversion-electron Mössbauer spectroscopy (CEMS) did detect surface crystallization beginning at $T_A = 660$ K.[15] Earlier, the development of an out-of-plane easy anisotropy direction was attributed to a stress-magnetostriction interaction produced by surface crystallization in $Fe_{82}B_{12}Si_6$,[19] $Fe_{40}Ni_{38}Mo_4B_{18}$,[20] and $Fe_{75.4}Si_{14.2}B_{10.4}$.[21] It is reasonable to propose that a similar mechanism acts in $Fe_{81}B_{13.5}Si_{3.5}C_2$.

C. Atomic rearrangements before bulk crystallization

The isomer shift δ, quadrupole shift ϵ, and the average linewidth of the amorphous phase are

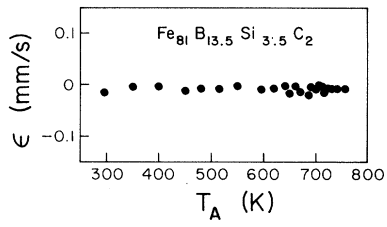

FIG. 11. Quadrupole shift as a function of annealing temperature of the amorphous component of $Fe_{81}B_{13.5}Si_{3.5}C_2$, determined from room-temperature spectra.

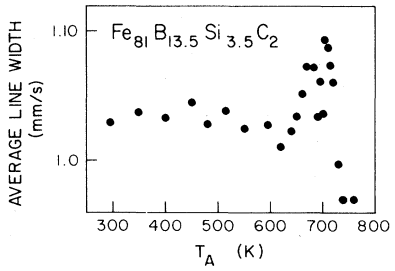

FIG. 12. Annealing temperature dependence of the average linewidth of the amorphous component at room temperature.

shown as a function of annealing temperature in Figs. 10, 11, and 12, respectively. The quadrupole shift is zero, within the experimental error, over the entire annealing-temperature range; therefore, the magnetic hyperfine field is randomly orientated with respect to the principal axes of the electric field gradient, as observed for the as-quenched ribbon.[5]

Since the original proposal by Chen and Coleman,[22] it is now generally accepted that annealing at temperatures well below that required for crystallization leads to atomic rearrangements within the amorphous alloy. Consideration of the annealing-temperature dependences of the hyperfine field (Fig. 7), the isomer shift (Fig. 10), the average linewidth (Fig. 12), and the total absorption area (Fig. 6), suggest that structural relaxation processes before the onset of bulk crystallization may be divided into three regions, viz, for T_A up to 400 K, for $400 \leq T_A \leq 620$ K, and for $620 < T_A < 690$ K. From the as-quenched alloy up to $T_A \approx 400$ K, little change occurs in the hyperfine parameters; consequently, no meaningful discussion can be given for this low annealing-temperature range.

1. $400 \leq T_A \leq 620$ K

The region in which the annealing temperature goes from 400 to 620 K is characterized by (a) an increase in the hyperfine field (Fig. 7), (b) a decrease in the isomer shift (Fig. 10), (c) a small decrease in the average linewidth (Fig. 12), and (d) probably a slight increase in the total absorption area. Now a previous investigation has established that when the metalloid concentration of amorphous Fe-Si is reduced, the hyperfine field increases and the isomer shift decreases.[23] Further, if the boron concentration in Fe-B is less, the magnetization, which is presumed to be proportional to the hyperfine field, is larger. Therefore, it is reasonable to suppose the hyperfine-field increase and isomer-shift decrease observed for $Fe_{81}B_{13.5}Si_{3.5}C_2$ is the result of a decrease in the charge transferred from the metalloid atoms to the iron atoms[24] brought about by atomic rearrangements that lead to an enhancement in the short-range order.

The origin of this increase in the short-range order could be either topological, in which the interatomic distances and angles change, or chemical, in which Fe-Fe pairs are produced in preference to Fe-metalloid pairs. For an amorphous $Fe_{40}Ni_{40}P_{14}B_6$ alloy, Egami[25] proposed that Fe-Fe pairing was favored. In addition, in a dispersion x-ray diffraction study, Egami[26] proposed that the change in the nearest-neighbor shell with structural relaxation is not a change in the relative distances, but a rearrangement among the atoms. Thus, the basic structural units, such as a tetrahedron, within the framework of the random packing-of-spheres model, are hardly affected by the relaxation except for slight distortions, but the relative configurations of such units are changed during the annealing. Certainly, if Fe-Fe pairs are preferentially produced, the average ^{57}Fe hyperfine field would be expected to increase and the isomer shift to decrease, as observed for $Fe_{81}B_{13.5}Si_{3.5}C_2$.

The apparent slight increase in the total absorption area (Fig. 6), which is proportional to the recoilless fraction, indicates that ^{57}Fe bonding becomes stronger. The decrease in the average linewidth of the six Mössbauer lines (Fig. 12), implies that the distribution of hyperfine parameters, especially the hyperfine field, becomes smaller. Both these results are consistent with the enhancement of short-range Fe-Fe pair ordering during isochronal annealing for $400 \leq T_A \leq 620$ K.

2. $620 < T_A < 690$ K

As the annealing temperature is increased from 620 to 690 K, the hyperfine field decreases (Fig. 7), the isomer shift has a maximum at about $T_A \approx 620$ K (Fig. 10), the average linewidth increases (Fig. 12), and the total absorption area increases more rapidly (Fig. 6). The lack of correlation between the hyperfine-field and isomer-shift changes would appear to rule out the earlier charge-transfer model. The increase in the hyperfine-field distri-

bution and increase in the strength of the atomic bonding, inferred from Figs. 12 and 6, respectively, suggest that atomic rearrangements are occurring that set the stage for crystallization. Indeed, although no bulk crystallization is observed in this annealing-temperature range, it is possible that some crystalline nucleation has developed. In any event, the atomic rearrangements taking place for $620 < T_A < 690$ K are of a different nature than those occurring for $400 \leq T_A \leq 620$ K. Since the first crystalline phase to appear is Fe—4 at. % Si, perhaps atomic rearrangements produce an atomic clustering that just precedes the formation of Fe-Si crystalline nuclei. It is interesting to note that in a recent positron-annihilation study of an amorphous $Fe_{40}Ni_{40}P_{14}B_6$ alloy,[27] it is proposed that structural relaxation takes place also in two stages.

IV. CONCLUSIONS

The transformations that occur in amorphous $Fe_{81}B_{13.5}Si_{3.5}C_2$ ribbon after isochronal annealing have been studied by ^{57}Fe Mössbauer spectroscopy. Before any bulk crystallization is detected, atomic rearrangements take place that may be classified into two stages. In the first stage, the formation of Fe-Fe pairs is favored. In the second stage, the precise details are uncertain, but it appears that the structural relaxation changes are the precursors to the onset of crystallization. Crystallization of the surface precedes that of the bulk; a study of surface crystallization is underway.

The first crystalline precipitate is Fe—4 at. % Si. After crystallization is completed the components are Fe—7 at. % Si, Fe_2B, and Fe_3C. During the crystallization process, two quasistable annealing-temperature ranges are observed. It would be of interest to investigate the transformations of $Fe_{81}B_{13.5}Si_{3.5}C_2$ when different annealing times are employed.

ACKNOWLEDGMENT

This research received financial support from the Natural Sciences and Engineering Research Council of Canada.

[1]K. Fukamichi, M. Kikuchi, S. Arakawa, and T. Masumoto, Solid State Commun. 23, 955 (1977); T. Kemény, I. Vincze, and B. Fogarassy, Phys. Rev. B 20, 476 (1979); T. Tarnoczi, I. Nagy, C. Hargitai, and M. Hosso, IEEE Trans. Magn. 14, 1025 (1978).

[2]A. S. Schaafsma, H. Snijders, and F. van der Woude, Phys. Rev. B 20, 4423 (1979).

[3]H. N. Ok and A. H. Morrish, Phys. Rev. B 22, 3471 (1980).

[4]D. C. Price, The Australian National University, Australia, Research Report No. 5 (unpublished).

[5]N. Saegusa and A. H. Morrish, Phys. Rev. B 26, 10 (1982).

[6]N. N. Greenwood and T. C. Gibb, *Mössbauer Spectroscopy,* (Chapman and Hall, London, 1971).

[7]C. E. Violet and D. N. Pipkorn, J. Appl. Phys. 42, 4339 (1971).

[8]J. D. Cooper, T. C. Gibb, N. N. Greenwood, and R. V. Parish, Trans. Faraday Soc. 60, 2097 (1964).

[9]L. Tákacs, M. C. Cadeville, and I. Vincze, J. Phys. F 5, 800 (1975).

[10]I. Vincze, D. S. Boudreaux, and M. Tegze, Phys. Rev. B 19, 4896 (1979).

[11]I. Vincze and I. A. Campbell, Solid State Commun. 14, 795 (1974).

[12]T. Ericsson, L. Häggström, and R. Wäppling, Phys. Scr. 17, 83 (1978).

[13]L. Häggström, L. Gränäs, R. Wäppling, and S. Devanarayanan, Phys. Scr. 7, 125 (1973).

[14]H. Bernas, I. A. Campbell, and R. Fruchart, J. Phys. Chem. Solids 28, 17 (1967).

[15]N. Saegusa and A. H. Morrish (unpublished).

[16]S. Arajs, R. Caton, M. Z. El-Gamal, L. Gránásy, J. Balogh, A. Gziraki, and I. Vincze, Phys. Rev. B 25, 127 (1982).

[17]J. C. Swartz, J. J. Haugh, R. F. Krause, and R. Kossowsky, J. Appl. Phys. 52, 1908 (1981); J. C. Swartz, R. Kossowsky, J. J. Haugh, and R. F. Krause, *ibid.* 52, 3324 (1981).

[18]N. S. Kazama, T. Masumoto, and M. Mitera, J. Magn. Magn. Mater. 15-18, 1331 (1980).

[19]H. N. Ok and A. H. Morrish, Phys. Rev. B 23, 2257 (1981).

[20]H. N. Ok and A. H. Morrish, J. Appl. Phys. 52, 1835 (1981).

[21]H. N. Ok and A. H. Morrish, J. Phys. F 11, 1495 (1981).

[22]H. S. Chen and E. Coleman, Appl. Phys. Lett. 28, 245 (1976).

[23]G. Marchal, Ph. Mangin, M. Piecuch, and Chr. Janot, J. Phys. (Paris) 37, C6-763 (1976).

[24]T. Mizoguchi, *Magnetism and Magnetic Materials—1976 (Joint MMM-Intermag Conference, Pittsburgh),* Partial Proceedings of the First Joint MMM-Intermag Conference, edited by J. J. Becker and G. H. Lander (American Institute of Physics, New York, 1976), p. 286; R. C. O'Handley and D. S. Boudreaux, Phys. Status Solidi A 45, 607 (1978).

[25]T. Egami, Mater. Res. Bull. 13, 557 (1978).

[26]T. Egami, J. Mater. Sci. 13, 2587 (1978).

[27]T. Mihara, S. Otake, H. Fukushima, and M. Doyama, J. Phys. F 11, 727 (1981).